atmosphere

MDPI

Article

Ozone Trends and the Ability of Models to Reproduce the 2020 Ozone Concentrations in the South Coast Air Basin in Southern California under the COVID-19 Restrictions

Lynsey Karen Parker, Jeremiah Johnson, John Grant, Pradeepa Vennam, Rajashi Parikh, Chao-Jung Chien and Ralph Morris *

Ramboll, 7250 Redwood Blvd, Suite 105, Novato, CA 94945, USA; lparker@ramboll.com (L.K.P.); jjohnson@ramboll.com (J.J.); jgrant@ramboll.com (J.G.); pvennam@ramboll.com (P.V.); rparikh@ramboll.com (R.P.); cjchien@ramboll.com (C.-J.C.)
* Correspondence: rmorris@ramboll.com; Tel.: +1-510-899-0708

Abstract: The current U.S. emission control requirements for on-road motor vehicles are driven by the ozone problem in the South Coast Air Basin (SoCAB) in southern California. Based on ozone modeling performed for Air Quality Management Plans (AQMPs), the SoCAB ozone attainment plan requires large (>80%) amounts of emission reductions in oxides of nitrogen (NOx) from current levels with more modest (~40%) controls on Volatile Organic Compounds (VOC). The shelter in place orders in response to the 2020 COVID-19 pandemic resulted in an immediate reduction in emissions, but instead of ozone being reduced, in 2020 the SoCAB saw some of the highest observed ozone levels in decades. We used the abrupt emissions reductions from 2019 to 2020 caused by COVID-19 to conduct a dynamic model evaluation of the Community Multiscale Air Quality (CMAQ) model to evaluate whether the models used to develop ozone control plans can correctly simulate the ozone response to the emissions reductions. Ozone modeling was conducted for three scenarios: 2019 Base, 2020 business-as-usual (i.e., without COVID reductions), and 2020 COVID. We found that modeled ozone changes between 2019 and 2020 were generally consistent with the observed ozone changes. We determined that meteorology played the major role in the increases in ozone between 2019 and 2020; however, the reduction in NO_X emissions also caused ozone increases in Los Angeles County and into western San Bernardino County, with more widespread ozone decreases further to the east.

Keywords: CMAQ; dynamic model evaluation; COVID-19; ozone; South Coast Air Basin (SoCAB)

Citation: Parker, L.K.; Johnson, J.; Grant, J.; Vennam, P.; Parikh, R.; Chien, C.-J.; Morris, R. Ozone Trends and the Ability of Models to Reproduce the 2020 Ozone Concentrations in the South Coast Air Basin in Southern California under the COVID-19 Restrictions. *Atmosphere* **2022**, *13*, 528. https://doi.org/10.3390/atmos13040528

Academic Editor: S. Kent Hoekman

Received: 28 January 2022
Accepted: 25 March 2022
Published: 26 March 2022

1. Introduction

In response to the COVID-19 pandemic, there have been substantial reductions in many activities (e.g., driving, manufacturing, goods movement) that generate ozone and fine particulate matter ($PM_{2.5}$) precursor emissions across the world. This has resulted in a real-world experiment of a sudden reduction in emissions that allows an assessment of how air quality responded to the reductions in emissions. Researchers seized the opportunity to study changes in air quality due to the COVID-19 pandemic, and numerous studies have been performed.

Seven months into the pandemic, Gkatzelis et al. [1] reviewed the scientific literature of accepted peer-reviewed journals of over 200 papers that studied air quality changes during the pandemic. Many of the studies focused on the analysis of ground-based and/or satellite observations and reported a range of findings depending on study parameters: period, global geographic region, urban versus rural focus, primary versus secondary pollutants, degree of spatial aggregation, and consideration of confounding factors such as long-term trends and/or meteorological influences. However, despite these differences, consistent patterns have emerged. For example, Bekbulat et al. [2] considered evidence from U.S. regulatory monitors and found that, in general, concentrations of ozone (O_3)

and nitrogen dioxides (NOx) were lowered, but the reduction was modest and transient. Their findings are important on regional scales but, because they spatially aggregated data, important local scale variations (e.g., within the South Coast Air Basin (SoCAB) of California) may be obscured in their analysis. Fu et al. [3] considered the Air Quality Index (AQI) in 20 major cities worldwide and found substantially decreased NO_2 concentrations and smaller, mixed impacts on ozone concentrations from COVID-19 lockdowns. For Los Angeles, they found lower NO_2 AQI but no noticeable effect on ozone AQI during their study period of 19 March–7 May 2020. Goldberg et al. [4] utilized TROPOMI satellite data to disentangle the impact of the COVID-19 lockdowns on urban NO_2 from natural variability and found that, after accounting for meteorology, NO_2 reductions were between 9.2% and 43.4% among 20 cities in North America, and approximately 33% in Los Angeles from 15 March to 30 April 2020. Venter et al. [5] utilized TROPOMI satellite data and ground-based observations and concluded that lockdown events have reduced the population-weighted concentration of nitrogen dioxide and particulate matter levels by about 60% and 31% in 34 countries, with mixed effects on ozone during lockdown dates up to 15 May 2020. Campbell et al. [6] evaluated the impacts of the COVID-19 lockdowns on emissions and ozone air quality by using observational data and the National Air Quality Forecasting Capability (NAQFC) air quality modeling system, which utilizes CMAQ at 12 km resolution. Their study included the entire U.S. and evaluated the period March–September 2020. They found variable impacts on maximum daily 8-hr average (MDA8 ozone concentrations across the U.S., including widespread decreases in rural regions but also localized increases near some of the highly populated urban areas

The impacts of COVID-19 on air quality have also been investigated with a modeling study by Gaubert et al. [7], who used the global Community Earth System Model (CESM v2.2, Boulder, CO, USA) to investigate the response of secondary pollutants (ozone, secondary organic aerosols) in different parts of the world in response to modified emissions of primary pollutants during the COVID-19 pandemic. They found ozone decreases for most of the U.S. but increases in ozone within the SoCAB as well as a few other localized regions.

Keller et al. [8] performed a global modeling study of the Global Impact of COVID-19 restrictions on the surface concentrations of nitrogen dioxide and ozone using a machine learning algorithm that is trained to predict and correct for the systematic (recurring) model bias between hourly observations and the collocated model predictions. These biases can be due to errors in the model, such as emission estimates, sub-grid scale local influences, or meteorology and chemistry. They found the COVID-19 ozone response to be complicated by competing influences of non-linear atmospheric chemistry and to be dependent on season, time scale, and environment.

Studies that focused on ozone in the SoCAB include Ivey et al. [9], who studied the impacts of the 2020 COVID-19 shutdown measures on ozone production in the Los Angeles basin. Their analysis was restricted to March and April of 2020 when daily activities were most restricted, and emissions reductions were greatest. This period generally has lower ozone concentrations compared to mid-summer and are of lesser importance as regards defining ozone attainment control plans. They found mixed ozone results, with overall increases in the upwind site at Pasadena and decreases in the downwind site at Crestline. Parker et al. [10] studied the impacts of traffic reductions associated with COVID-19 on Southern California Air Quality and found an overall reduction in NOx across the basin and moderate levels of mixed changes in O_3 concentrations, which suggests to them that additional mitigation approaches besides on-road NOx emissions reductions will be necessary to comply with air quality standards.

The common thread in these studies is that NOx decreased in response to COVID-19 restrictions and O_3 showed mixed results. The O_3 response was generally location dependent and increased within urban regions, which is consistent with the expected ozone response to reductions in NOx within VOC-limited regions. In our study, we use the COVID-19 emissions reductions for two purposes:

1. To perform a dynamic model evaluation of the Community Multiscale Air Quality (CMAQ) [11] modeling system to evaluate whether CMAQ correctly predicts the ozone air quality response to the COVID-19 emissions reductions for the SoCAB;
2. To assess the impact of the COVID-19 emissions reductions on ozone in the SoCAB with the CMAQ model.

Dynamic model evaluations are recommended by Dennis et al. [12] as one of four types of evaluations within their proposed model evaluation framework. The other three types of evaluations are: operational, diagnostic, and probabilistic. The operational evaluation has been standardized, and there is an Environmental Protection Agency (USEPA) Atmospheric Model Evaluation Tool (AMET) [13] that aids with operational model evaluations. The EPA also states that a dynamic evaluation is always recommended but acknowledges that the needed measurements and resources may not be available and that there are additional challenges, such as identifying appropriate case studies [14]. The COVID-19 emissions reduction scenario is such a case study because there was an abrupt emissions change over a short time scale and the requisite meteorological and air quality observational data are readily available. Thus, this real-world experiment can provide insight into whether the CMAQ model—which is used to predict future-year ozone air quality in regulatory planning—can correctly simulate the ozone response to the emissions reductions. A correct response is critical to ensure that appropriate control measures are applied to attain the National Ambient Air Quality Standards (NAAQS).

Karamchandani et al. [15] recently performed a dynamic model evaluation of the CMAQ model for the SoCAB region. They used two recent South Coast Air Quality Management District (SCAQMD) databases, used to define ozone control plans for the SoCAB, to evaluate the ability of CMAQ to reproduce the observed changes in ozone from 1990 to 2014/2015. They found that CMAQ tended to under-predict ozone responses by as much as a factor of two in recent years for the Basin maximum ozone design.

Our dynamic model evaluation found that the modeled ozone changes between 2019 and 2020 were generally consistent with the observed ozone changes using procedures that are used to make future-year ozone projections (which lends confidence to the projections procedures). We determine that meteorology played the major role in the increases in ozone between 2019 and 2020; however, the NO_x emissions reductions due to COVID-19 caused ozone increases in Los Angeles County and into western San Bernardino County, with ozone decreases more widespread further east, which indicates that ozone formation in parts of the SoCAB is still VOC-sensitive. Note that we did not apply COVID-19 adjustments to background ozone that is transported into the region through model boundary conditions; this limitation is discussed in more detail later. This study highlights the fact that the evaluation of VOC/NO_x emission control strategies to attain the ozone NAAQS needs to examine ozone levels in the intervening years between the current and the attainment year to better understand whether ozone may be getting worse or cause more population exposure to high ozone concentrations, rather than focusing exclusively on ozone levels in the attainment year.

2. Materials and Methods

We selected the study period to satisfy multiple criteria: (1) measurable emissions changes due to COVID-19 restrictions; (2) regulatory significance for ozone formation potential (i.e., includes days with ozone close to the current year ozone design values), (3) meteorologically non-anomalous conditions, (4) absence of confounding factors such as wildfires. Google mobility data [16] indicated that the largest effect on transportation occurred in late March and April, with a lessening but continued effect as the summer progressed. In addition, TROPOMI and OMI [17] satellite NO_2 column data indicated that NO_2 columns were lower in June and July than in previous years for the SoCAB, even after considering meteorology and non-COVID related trends [14,18]. Note that Qu et al. [19] performed a study that utilized surface NO_2 measurements during the COVID-19 shutdown to evaluate the appropriateness of using the satellite NO_2 column to infer NOx emissions

trends. They found the satellite NO_2 columns generally showed a muted response compared to surface measurement due to the background NO_2 contribution. However, for regions with the highest levels of surface NO_2, the satellite data can capture the magnitude of the NOx emissions reductions from March to June 2020. We analyzed the regional meteorology for the period May–August 2020, including the 850 mb temperature (T850), which is the most descriptive parameter for determining the ozone formation potential in the SoCAB. High T850 gives an indication of the strength of the temperature inversion that can trap pollutants near the surface as well as the presence of high temperatures and slow wind speeds, all of which lead to higher ozone formation. We found that May 2020 had much higher T850 than the previous five years, especially May 2019, which was wet and cold, and August 2020 had higher monthly T850 than the previous five years. In addition, August 2020 had an intense wildfire season throughout California [20]. For these reasons we restricted our modeling and analysis to June and July 2020. We also modeled June and July 2019 to perform the dynamic model evaluation.

The modeling component of this study was accomplished with the WRF meteorological model and the CMAQ photochemical grid air quality model. The WRF and CMAQ 12-km and 4-km modeling domains are displayed in Figure 1a, along with the domain parameters. Figure 1b is a closer look at the SoCAB study region, with ozone monitors indicated and counties labeled. The model projection is Lambert Conic Conformal with latitude of origin = 37.0 N, Central Meridian 120.5 W, and Standard Parallels at 30.0 N and 60.0 N.

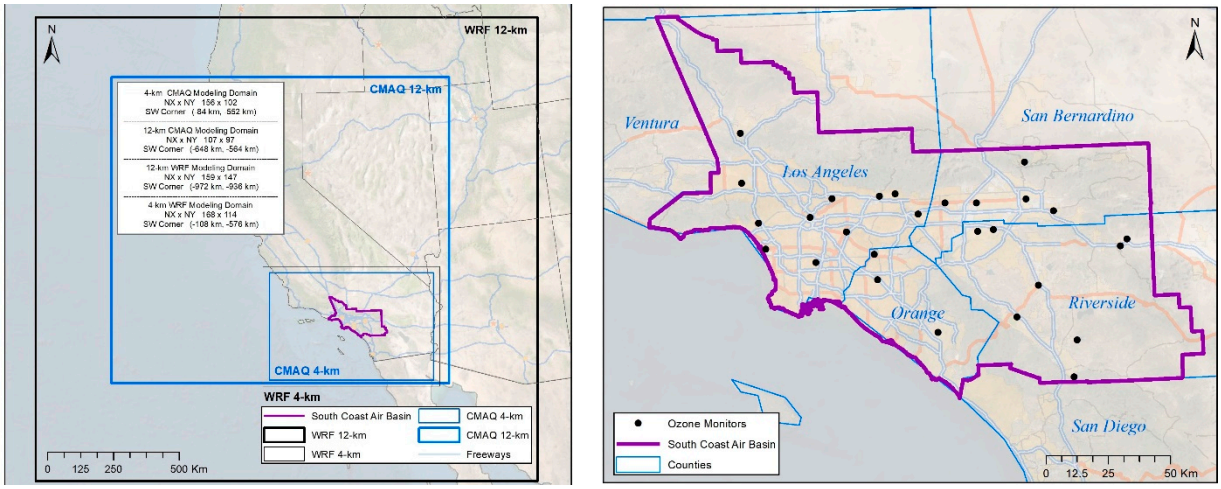

(**a**) (**b**)

Figure 1. Study area: (**a**) Geographic extents and modeling domain parameters; (**b**) South Coast Air Basin study region with monitor locations and SoCAB counties.

2.1. WRF Meteorological Modeling and Model Performance

WRF was used to generate meteorological conditions and inputs for the 4-km and 12-km domains for the mid-May through July period in 2019 and 2020, where mid-May–June 1 is the spin-up period. WRF physics options, performance thresholds, and performance for the 4-km WRF simulations for select surface sites and upper air sites is provided in the Supplementary Information Document, Section S1. The WRF model performance was typical for a good WRF application. The Meteorology—Chemistry Interface Processor (MCIP) [21] was used to process the WRF output for CMAQ.

2.2. Emissions Inventories and Processing

Anthropogenic emissions for California were from the ARB 2020 emissions inventory (EI) [22]. These emissions are available in a "pre-merged" format, which means they

are stored by individual source sectors (e.g., on-road, aircraft), which facilitates applying different COVID-19 scaling factors to the different emissions source sectors. Biogenic emissions were based on the Model of Emissions of Gases and Aerosols From Nature (MEGAN) v3.1 biogenic emissions model [23] with ARB's adjusted urban leaf area index (LAI) using 12/4-km WRF meteorological data. Fire emissions were based on the Fire INventory from NCAR (FINN) [24]. Emissions for the Mexico region in the 4 km domain were from the South Coast Air Quality Management Plan (2016 AQMP) EI [25]. Figure 2 displays the anthropogenic by-sector emissions breakdown for the SoCAB for the ARB 2020 EI. Any sector with less than 1% contribution to the total is not displayed. The period-average is for the period 1 June–31 July 2020.

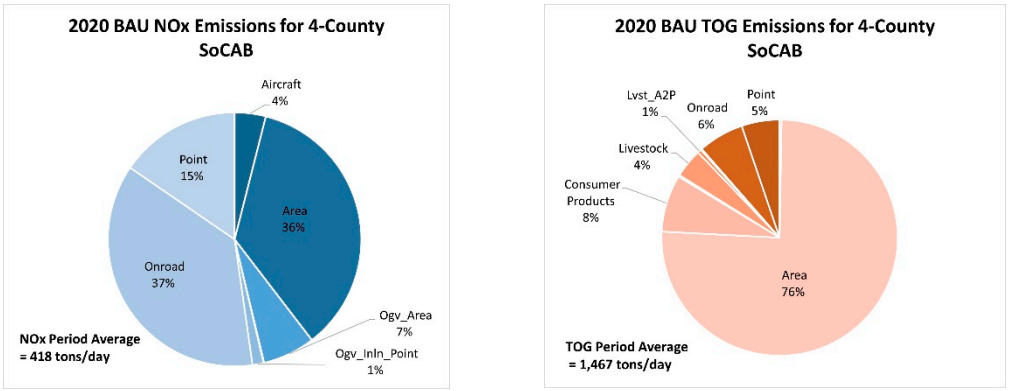

(**a**) (**b**)

Figure 2. Four-county South Coast Air Basin 2020 BAU emissions by sector: (**a**) NOx emissions; (**b**) TOG emissions.

We developed model-ready emissions for three CMAQ scenarios:

1. 2019 Base Case;
2. 2020 BAU Case;
3. 2020 COVID Case.

The 2019 Base emission were obtained by scaling the ARB 2020 EI. We inspected the 2019 and 2020 California Emissions Projection Analysis Model (CEPAMS) [26] summertime grown and controlled emissions for the South Coast Air Basin by source sector and found that only on-road was a substantially contributing source (i.e., >3%), with a substantial (i.e., >± 5%) year-to-year change for any pollutant [26]. Therefore, we kept all sectors besides on-road at the same emissions rate in 2019 as in 2020 and adjusted the on-road sector only. The CEPAM on-road 2019 adjustment factors are as follows: NOx = 1.11, TOG = 1.07, and CO = 1.10. These factors were applied uniformly over the 4-km domain to the on-road emissions for each hour.

2020 BAU emissions were taken directly from the ARB 2020 EI without any scaling adjustment because these emissions we compiled prior to the pandemic and do not account for pandemic effects. The pre-merged categories that comprise this inventory are:

- Aircraft;
- Area source;
- Consumer products;
- On-road;
- Point (point source format);
- Fertilizer;
- Livestock;
- Lvst (a2p);
- Ogv Area;
- Ogv Inln (point source format);

- Ogv military;
- Paved;
- Residential Wood Combustion;
- Unpaved.

OGV is ocean-going vessels, and Lvst is a second livestock category. Off-road emissions (e.g., construction equipment) are included in the area source category.

2.2.1. 2020 COVID Emissions Adjustments

A bottom-up approach was employed to adjust the 2020 BAU emissions with source sector-specific COVID adjustment factors based on changes in activity. For some sectors, adjustments were developed at a more disaggregated level, namely by Source Classification Codes (SCCs), e.g., within on-road for heavy duty and light duty vehicles, using auxiliary information available within the ARB 2020 EI to determine fractions of subcategories within a sector. Detailed information regarding the data sources utilized, activity basis, geographic and temporal specificity, and derived adjustment factors is provided in the Supplementary Information Document, Section S3. The sector with the largest NOx reductions is on-road, and the primary data source used to derive the on-road scaling factor was the U.S. Energy Information Administration (EIA) refinery gasoline and diesel sales in California. EIA June and July 2020/2019 fuel sale ratios were 77% for gasoline and 84% for diesel. ARB's Emission FACtor (EMFAC) tool [27] was used to calculate Vehicle Miles Traveled (VMT) and appropriately apply scaling factors to the on-road fleet. Figure 3 provides a summary of the emissions for the three model scenarios for NOx and TOG in panels (a) and (b), respectively. Note that the TOG emissions adjustments are less than 1% between the three scenarios, because they are dominated by area sources that had a minimal COVID adjustment, and the change in on-road VOC (−27.2 tpd) is partially offset by an increase in the consumer products (+12.1 tpd).

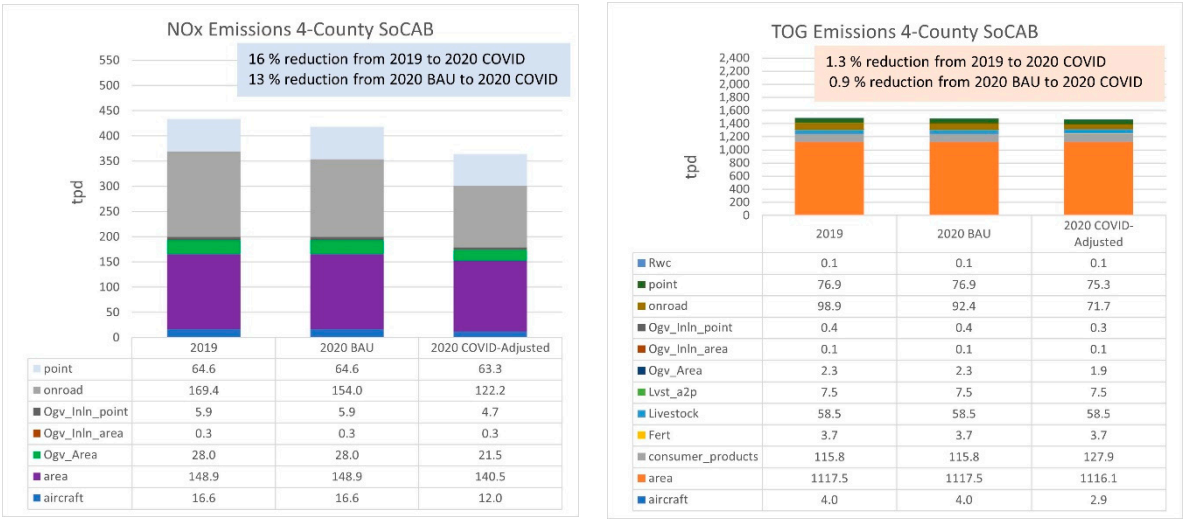

(**a**) (**b**)

Figure 3. Four-county South Coast Air Basin 2019, 2020 BAU, and 2020 COVID emissions comparison by sector: (**a**) NOx emissions; (**b**) TOG emissions.

2.2.2. Emissions Processing for Model-Ready Emissions

The 2019 and 2020 adjustment factors were applied to the pre-merged 2020 BAU emissions files. Figure 4 presents examples of the spatial distribution of the merged gridded NOx emissions (NOx ≈ NO + NO_2) for 10 June 2020, at 0:00 UTC in moles/s per 4-km grid cell. Figure 4a is 2020 BAU and Figure 4b is the 2020 COVID/2020 BAU ratio (unitless). Note that the conversion factor from moles/s to tons/day for NOx is 4.38.

Figure 4a shows that the highest NOx emissions come from the Los Angeles region as well as along the coast to San Diego. Figure 4b shows that NOx reductions are approximately 8% over the Pacific due to the OGV reductions and shows a range of reductions throughout the domain and approximately a 10–15% reduction over the SoCAB. For Mexico, the 2020 BAU/2020 COVID ratio is one since those emissions were unadjusted.

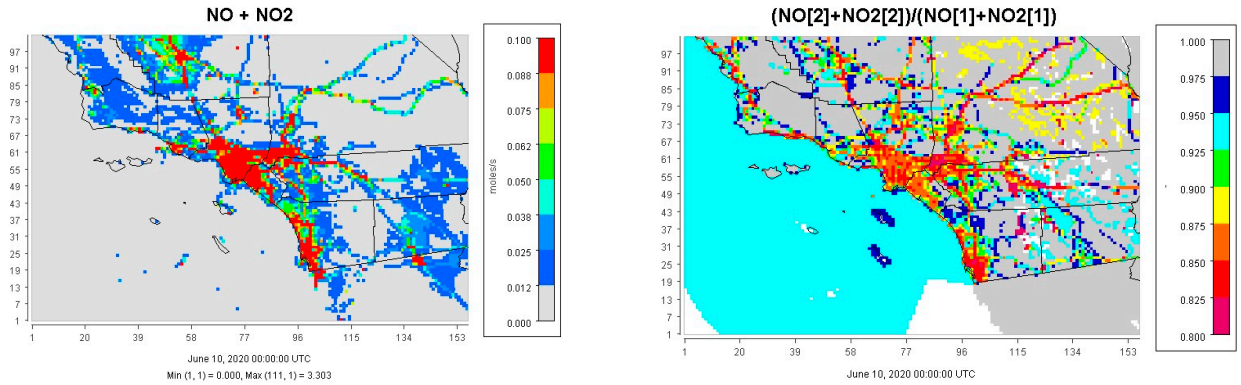

(**a**) (**b**)

Figure 4. Example of model-ready NOx emissions on the 4-km domain: (**a**) 2020 BAU NOx emissions; (**b**) 2020 BAU/2020 COVID NOx emissions.

2.3. CMAQ Model Configuration

CMAQ version 5.2.1 was run from June through July (with a 10-day spin-up in May) for the 12-km and 4-km modeling domains for 2019 and 2020 for the emissions scenarios previously described. The 12-km simulation results were used solely to derive boundary conditions (BC) for the 4-km simulations. We used the same 2020 12-km BC simulation for both 2020 4-km simulations and the 2019 12-km BC simulation for the 2019 4-km simulation. BCs for the 12-km simulations were from the Whole Atmosphere Community Climate Model (WACCM) [28], which has 2019 and 2020 model output available, which was utilized for the 2019 and 2020 12-km CMAQ simulations, respectively. Both the 12-km and 4-km simulations used the same science options that are provided in the Supplementary Information Document, Section S2. The model was run on a multi-processor machine with 24 processors (6 NCOLS $\times$ 4 NROWS).

2.4. CMAQ Operational Model Performance Evaluation

The AMET tool was used to evaluate the CMAQ simulations using concurrent ozone observations. Model performance statistics (i.e., bias, error, and correlation) and time series plots were calculated at monitoring sites. Scatter plots of predicted and observed concentrations were generated as well as spatial maps of site-specific performance statistics. Emery et al. [29] provide a set of statistics and benchmarks to assess PGM performance. They deemed that normalized mean bias (NMB) and error (NME) and correlation (r or COR) statistics have the best characteristics historically. Table 1 presents the statistical measures and goal and criteria thresholds for ozone for NMB, NME, and COR. Goal thresholds represent the statistical values that approximately one-third (i.e., the 33rd percentile) of top performing past applications have achieved and are considered the best a model can be expected to achieve. The less restrictive criteria are around the 67th percentile and indicate statistical values that approximately two-thirds of past applications have met. Additional relevant recommendations include: (1) no minimum cutoff for maximum daily 8-h average (MDA8) ozone; (2) temporal scales for ozone statistics should not exceed 1 month; and (3) spatial scales should range from urban to $\leq$1000 km.

Table 1. Statistical measures, goal and criteria thresholds for ozone model performance. Excerpted from Emery et al. [29].

Statistic/Abbreviation	Definition [1]	Notes
Normalized Mean Bias (NMB)	$\frac{\sum(P_j - O_j)}{\sum O_j} \times 100$	$-100\% \leq$ NMB $\leq +\infty$
Normalized Mean Error (NME)	$\frac{\sum\lvert P_j - O_j\rvert}{\sum O_j} \times 100$	$0\% \leq$ NME $\leq +\infty$
Correlation Coefficient (r)	$\frac{\sum[(P_j - \overline{P}) \times (O_j - \overline{O})]}{\sqrt{\sum(P_j - \overline{P})^2 \times \sum(O_j - \overline{O})^2}}$	Unitless, $-1 \leq$ r $\leq +1$ r = 1 is perfect correlation r = 0 is totally uncorrelated

Minimum Metrics and Benchmarks

	NMB		NME		r	
Species	Goal	Criteria	Goal	Criteria	Goal	Criteria
1-hr or MDA8 Ozone	$<\lvert\pm 5\%\rvert$	$<\lvert\pm 15\%\rvert$	<15%	<25%	>0.75	>0.50

[1] Subscript *j* represents the pairing of *N* observations and *O* predictions by site and time. Overbars signify means over the site and/or time.

Figure 5a shows scatter plots of MDA8 ozone performance for all sites in the 4-km domain for June and July for 2019 and 2020 COVID. The *x*-axis is observed MDA8 ozone, and the *y*-axis is CMAQ MDA8 ozone. Each point represents MDA8 ozone for one site on one day. NMB and NME are displayed in Figure 5a. For each case, the NME is between 15.9% to 17.1%, which easily meets the performance criterion and nearly meets the criteria goal. NMB has more variation between the four cases. For 2019, there is a positive NMB of 5.5% in June and a negative bias of −4.3% in July; these values are close to the performance goal. For 2020, there is a positive NMB of 9.6% in June and 1.5% in July. For both years, July exhibits a discernable negative bias at the higher range of observed MDA8 (e.g., >80 ppb). Figure 5b presents spatial plots of site-specific NMB and NME statistical performance metrics for 2019 Base and 2020 COVID. For June, the majority of SoCAB monitors meet the NMB criteria, and all sites meet the NME criteria in both 2019 and 2020. For July, there is an underestimation bias at many monitors in the SoCAB in both 2019 and 2020, but the NME falls within the criteria. Outside of the SoCAB, CMAQ tends to overestimate ozone for both months and both years at some sites.

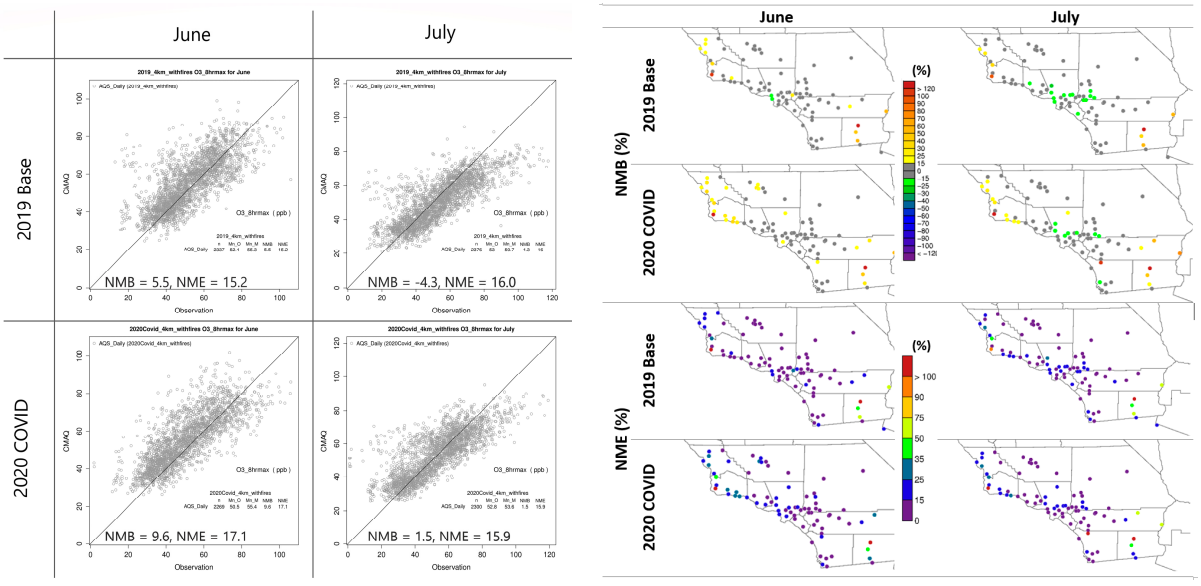

(**a**) (**b**)

Figure 5. MDA8 ozone performance plots: (**a**) Scatter plots; (**b**) Spatial plots of NMB and NME.

The SI (Section S4) presents additional performance statistic on a per monitor basis, including timeseries plots and statistics tables for ten selected sites that span the SoCAB. As an example, three timeseries plots are shown in Figure 6 (the location of these three sites can be found in a later section). Note that differences between the 2020 COVID and 2020 BAU timeseries plots shown in the right panels of Figure 6 are small and overshadowed by day-to-day variations; these small differences are consistent with the spatial plot results shown later. The statistics tables in SI Section S4 and the time series plots show that, for both 2019 and 2020, NMB performance is superior in June (most sites meet the NMB goal) compared to July (negative bias at all but one site and many sites do not meet the criteria). Investigating why the July performance is inferior to June was beyond the scope of this study, but we note that the period-wide highest days are mostly in July and the CMAQ model does not fully capture the highest days. A similar phenomenon is observed in the SCAQMD 2016 AQMP [25] performance for the "Urban Receptor" monitors that correspond to the San Bernardino monitors, where the negative bias is more severe in July than in June. Overall, ozone model performance was generally within typical thresholds based on historical PGM applications.

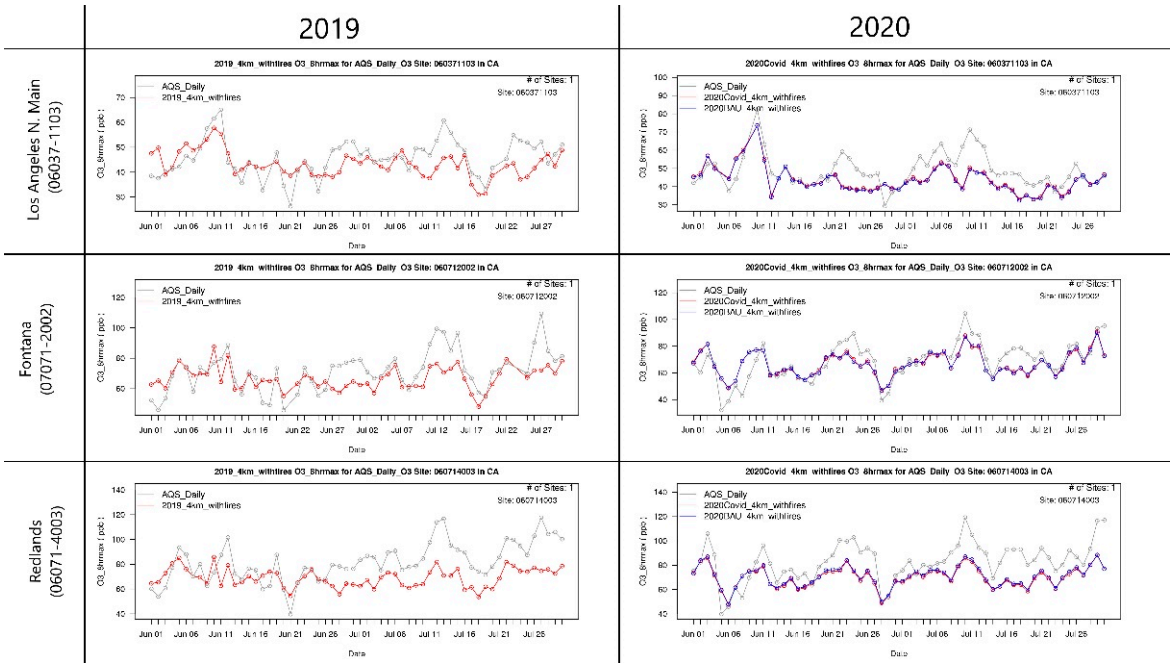

Figure 6. Example timeseries plots for 2019 and 2020 for Los Angeles N Main, Fontana, and Redlands monitors.

We do not present a NOx model performance analysis because the operational AMET products for nitrogen species may fail to give meaningful results because most commercial NOx analyzers do not measure true NO_x. Instead, they measure NOγ where NOγ = NO_x + nitrous acid (HONO) + nitric acid (HNO_3) + others nitrogen species; therefore, as Dickerson et al. [30] point out, standard NOx evaluations may involve errors of a factor of two or more. There are approaches to reduce the impact of the interfering species by focusing on early morning hours when the NOx species are expected to dominate the NOγ, as per Toro et al. [31], which we recommend for future work.

We performed a fire emissions sensitivity test for the 2020 COVID case by eliminating fire emissions (i.e., we performed a "zero-out" simulation) and found that during the June–July 2020 period fire impacts on ozone concentrations were negligible.

2.5. Evaluation Approach

Recall that this study had two main goals: (1) to perform a dynamic model evaluation of the CMAQ model to determine whether it can reproduce the observed ozone response due to the sudden emissions reductions associated with the COVID-19 pandemic; and (2) to examine the impacts of the COVID-19 emissions reductions in the SoCAB with CMAQ. The first goal is accomplished by considering the two scenarios that occurred (i.e., 2019 Base and 2020 COVID) and comparing the modeled responses and observed ozone responses. The second goal is accomplished by comparing the two 2020 modeled scenarios (i.e., 2020 COVID and 2020 BAU).

2.5.1. Dynamic Evaluation Methodology

For the dynamic evaluation, we follow the EPA modeling guidance procedures [14] for projecting ozone concentrations in an ozone model attainment demonstration. This approach was used in the SCAQMD's AQMP [25] to define ozone attainment VOC/NOx emission control strategies. The 2020 COVID Case represents the future-year emissions scenario, and 2019 Base Case represents the base year. Typically, the future year for a model attainment demonstration may be five or more years in the future (or a decade or more for the SoCAB extreme ozone NAA), but the abrupt emissions reductions due to COVID-19 restrictions mimic a potential future-year scenario and has the unique attribute of having observations for the comparison. In a typical model attainment demonstration, the meteorology is the same for the future and base years because the future-year meteorology is unknown. For this analysis, however, the meteorology is different between 2019 and 2020, although the June–July 2019 and 2020 modeling periods were selected to have similar meteorology. The EPA recommends using model estimates in a relative rather than absolute sense to reduce potential model bias effects for making future-year ozone projections. Fractional changes in air pollutant concentrations between the model future-year and model-base-year are calculated; these ratios are called relative response factors (RRFs). The RRFs are multiplied by base-year-observed ozone concentrations to predict future-year ozone concentrations. The base-year observations are the average of three-years of design values (DVB; defined below), and the future-year ozone design value (DVF) projection formula is as follows:

$$DVF_i = RRF_i \times DVB_i, \quad (1)$$

where DVF_i is the estimated design value for the future year in which attainment is required at monitoring site i; RRF_i is the relative response factor at monitoring site i; and DVB_i is the base design value at monitoring site i.

We calculate RRFs as one would do for projecting future-year ozone design values, only instead of using modeling results for a base- and future-year emissions scenario with the same meteorological inputs, we use the modeling results for the 2019 Base Case and 2020 COVID Case that have different meteorology. We also calculate observation-based RRFs using the 2019 and 2020 ozone observations in a consistent fashion. We do not use the design values in our analysis because we only model 2 months, which is not long enough to define design values, therefore we only focus on the RRFs.

There are additional considerations for the RRF calculations regarding which days to use in the RRF calculation, and EPA guidance has evolved over the years. We follow the current EPA recommendation, which is to calculate RRFs based on the 10 highest modeled days in the base year. This is to reflect the fact that design values are based on the three-year average 4th high observed MDA8 ozone values. The EPA recommends "*selecting a set of modeled days that are likely to encompass a range of values that are somewhat higher than and somewhat lower than the 4th high value . . . this balances the desire to have enough days in the RRF to generate a robust calculation, but not so many days that the RRF does not represent days with concentrations near the observed design values*" [14]. We follow EPA recommendations to evaluate CMAQ using the standard regulatory procedures so that the results are relevant to the regulatory community. The EPA describes an additional basis for their guidance and reports that "*model response to decreasing emissions is generally most stable when the base ozone*

predictions are highest. The greater model response at higher concentrations is likely due to more "controllable" ozone at higher concentrations . . . In most urban areas, on days with high ozone concentrations, there is a relatively high percentage of locally generated ozone compared to days with low base case concentrations. Days with low ozone concentrations are more likely to have a high percentage of ozone due to background and boundary conditions." There are additional EPA specifications regarding the MDA8 ozone value (i.e., ≥60 ppb) and the number of days that meet that criterion. In our analysis, that criterion is generally met, but for monitors that do not meet the minimum number of days ≥ 60 ppb threshold, we proceed with the analysis with MDA8 < 60 ppb. In addition, we use a single-grid cell rather than the 3 × 3 array recommended by the EPA. Our procedure is as follows:

1. For 2019 Base and 2020 COVID, identify the top 10 (T10) modeled days for MDA8 ozone and calculate the average of those days;
2. For 2019 and 2020, calculate the average observed MDA8 ozone on the T10 modeled days;
3. Calculate RRFs as the ratio of 2020 COVID to 2019 Base for modeled T10 MDA8 ozone and observed T10 MDA8 ozone.

We do this for each SoCAB grid cell that contains a monitor to obtain a modeled/observed pair of RRFs at each monitoring site. In addition, for all model grid cells we calculate T10 modeled RRFs over all the SoCAB grid cells. In general, the T10 days may be different at each grid cell.

2.5.2. T10 Days Standard MPE

Prior to the dynamic model performance evaluation, we examined the model performance for the T10 modeled days that are used to calculate the RRFs. Figure 7 presents a scatter plot of observed versus modeled MDA8 for each day in the T10 modeled days at each monitoring site for 2019 and 2020 in panel (a) and (b), respectively. These points are a subset of the data in Figure 5a. Considered across all sites, the model performance is similar between the two years and has a similar underestimation bias that almost achieves (−6.3% in 2019) or does achieve (−4.0% in 2020) the ozone performance goal for NMB (±5%), with NME achieving the performance goal in both years (<15%). However, the model underestimates the highest observed MDA8 ozone concentrations. Model performance statistics for the selected sites is shown in Table 2.

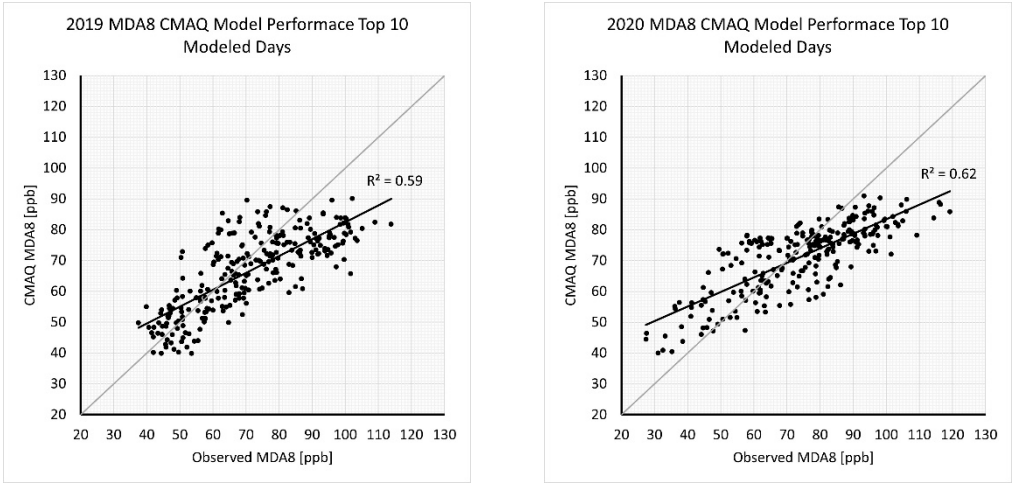

(**a**) (**b**)

Figure 7. Model performance scatter plots of the T10 modeled days: (**a**) 2019 Base; (**b**) 2020 COVID.

Table 2. NMB and NME for the T10 modeled days used in the RRF calculations [1].

Selected Sites	AQS Number	2019		2020	
		NMB (%)	NME (%)	NMB (%)	NME (%)
LAX	06-037-5005	−11.8	13.3	30.3	30.3
Los Angeles Main	06-037-1103	2.2	10.2	−2.1	10.8
Azusa	06-037-0002	−10.8	11.5	−5.4	13.2
Glendora	06-037-0016	−12.0	12.4	−13.1	16.0
Pomona	06-037-1701	19.4	20.3	−6.4	11.7
Upland	06-071-1004	−6.0	12.8	−8.2	12.1
Fontana	06-071-2002	−7.0	10.3	−1.3	10.1
Crestline	06-071-0005	−12.3	15.5	−10.2	12.3
San Bernardino	06-071-9004	−12.7	16.6	−12.7	14.4
Redlands	06-071-4003	−15.7	19.0	−17.6	17.8

[1] Values that failed to meet the criteria are highlighted in red.

3. Results

3.1. Dynamic Evaluation Based on RRFs

We present the results of the dynamic evaluation of the CMAQ model with standard projection procedures (i.e., based on RRFs) that are used for model attainment demonstrations in this section. Figure 8 is a spatial plot that compares gridded CMAQ RRFs with observed RRFs at monitoring sites across the SoCAB. Over much of the SoCAB, the modeled and observed RRFs are consistent and estimate that T10 modeled day ozone increased between 2019 and 2020 with some exceptions: (1) The two monitors furthest east in the SoCAB (Banning Airport and Morongo), where both the modeled and observed RRFs agree that ozone is reduced; (2) Sites near the coast (e.g., West LA, LAX, and Compton), where the model estimates ozone increases (RRF > 1.15), while the observed RRFs decreased; (3) At five additional locations throughout the basin, where both modeled and observed changes were small to moderate but may change in the opposite direction (i.e., Crestline and Perris, where the model estimates essentially no change in the RRFs and the observed RRFs indicate a slight reduction; Azusa and Reseda, where the observed RRFs indicates no change and the model estimates a 5–10% increase; and, Fontana where observed RRF indicates a decrease of 2–5% and the model estimates an increase of 2–5%).

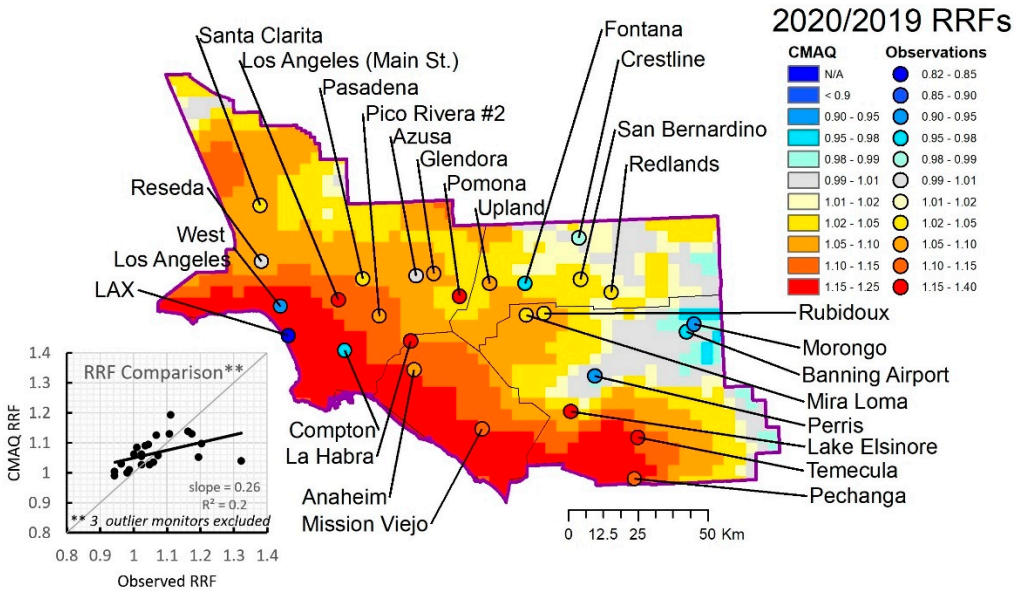

Figure 8. Comparison of CMAQ versus observed RRFs based on T10 modeled MDA8 ozone days.

Thus, the only monitors that indicate a regionally consistent and substantial discrepancy between the modeled and observed RRFs are the three southwestern Los Angeles County sites near the coast (i.e., West LA, LAX, and Compton). Some potential reasons for this are discussed below. Besides these three sites, there is general agreement between CMAQ and the observed ozone responses as shown in the scatter plot in Figure 8, which compares the observed and modeled RRFs, excluding the three coastal sites discussed above. This suggests that CMAQ is broadly able to replicate the observed ozone increase between 2019 and 2020 (that include the COVID-19 emissions reductions) within the framework of the EPA's recommended ozone projection procedures used in a modeled attainment demonstration. In general, the model response is weaker than the observed response (i.e., for monitors with the most extreme positive or negative observed responses (RRF > 1.15 and RRF < 1.0) the modeled response is muted), and responses at individual sites may vary (R^2 = 0.2). An obvious difference in modeled/observed RRFs is seen in the far-right side of the scatter plot in Figure 8 for the Pomona site, where the observed ozone increase (RRF = 1.32) is much greater than the modeled ozone increase (1.04). Note that the average modeled and observed RRFs in the scatter plot are both 1.07, which indicate a 7% increase in 2020 compared to 2019.

Poor RRF agreement at the LAX site can be traced to the general model performance for the T10 modeled days, as shown in Table 2, where 2019 had a modest negative NMB (–12%) and 2020 exhibited as extreme overestimate (30%) bias. Reasons for the poor performance at LAX potentially include meteorology, specifically the representation of the coastal marine layer in the WRF fields, and/or BCs from the WACCM global chemistry model.

3.1.1. Emissions Reduction Versus Meteorological Impacts on Ozone

Note that the analysis in Figure 8 has year-specific meteorology for the two years in the RRF calculations. Although the modeling periods of June–July 2019 and 2020 were selected to obtain modeling episodes in two different years with similar meteorology, there will still be differences, and the extent to which the meteorology affected the increase in ozone between 2019 and 2020 is investigated next.

Figure 9 compares two sets of modeled RRFs. Figure 9a is the same as Figure 8 (i.e., 2020 COVID/2019 Base) and Figure 9b is 2020 COVID/2020 BAU (which has emissions reductions but the same meteorology for both cases). Note that the 2020 BAU NO_x emissions are approximately 4% lower than the 2019 Base emissions (i.e., the RRFs in Figure 9a are based on a 17% difference, whereas Figure 9b is based on a 13% difference between the scenarios), so it is not a perfect one-to-one comparison; nevertheless, it is useful to get a sense of the relatively magnitude of meteorological versus emissions impacts. RRF deviations from unity for the dynamic meteorological case (i.e., Figure 9a) compared to the static meteorological case (i.e., Figure 9b) are much larger, which suggest that meteorology plays the dominant role in causing higher ozone in 2020 than in 2019. In addition, the spatial pattern is quite different between the two figures. Figure 9b shows regions of VOC-sensitive (yellow) and NO_x-sensitive (blue) ozone formation chemical regimes clearly delineated. This will also be seen in the next section.

3.1.2. Dynamic Model Evaluation Summary

We conclude that throughout the SoCAB (excluding the region of the three sites near the coast), CMAQ can replicate the observed ozone response to the COVID-19 emissions reductions and changes in meteorology between 2019 and 2020 within the framework of the ozone projections procedures used in a modeled ozone attainment demonstration. The modeled ozone response is weaker than the observed response, with substantial site-to-site variations. The modeled and observed ozone response between 2019 and 2020 was mainly an increase in ozone throughout most of the SoCAB, except in the eastern-most regions of the modeling domain (e.g., Banning Airport), where small decreases were observed and modeled. Analysis of the modeled ozone changes using the ozone projection procedures using static meteorology revealed much smaller ozone changes, which suggests

that differences in the 2019 and 2020 meteorology was a bigger driver for the increased ozone in 2020 than the chemistry due to the COVID-19-caused emission reductions.

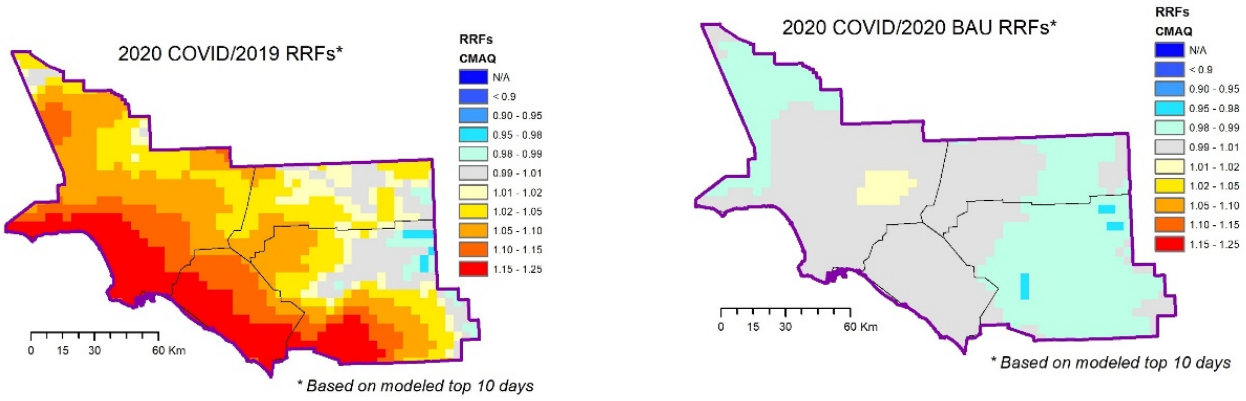

(**a**) (**b**)

Figure 9. CMAQ derived RRFs: (**a**) 2020 COVID/2019 Base; (**b**) 2020 COVID/2020 BAU.

3.2. Impacts of the COVID-19 Emissions Reductions on Ozone

Next, we present the CMAQ-predicted impacts of the COVID-19 emissions reductions on ozone concentrations. The left column of Figure 10a shows the 1 June–31 July period-average, period-maximum, and period-minimum MDA8 ozone for the 2020 COVID scenario in the upper, middle, and lower panels, respectively. Average MDA8 ozone greater than 70 ppb occurs in the western region of San Bernardino County and extends a little into eastern Los Angeles County.

The right column of Figure 10a shows the 1 June–31 July period-average, period-maximum, and period-minimum of the daily differences between 2020 COVID and 2020 BAU MDA8 ozone (i.e., the impacts of the COVID-19 emissions reductions) in the upper, middle, and lower panels, respectively. Grey represents minimal differences; cool shades represent ozone decreases and warm shades represent ozone increases. The period-maximum plot shows that in Los Angeles County and part of San Bernardino County ozone increases of greater than 2 ppb occurred at some time during the period. The period-minimum plot shows that throughout most of the domain (with a notable exception of the southeast quadrant of Los Angeles County) ozone decreases occurred and decreases of at least 1.5 ppb were widespread. The period-average difference plot domain-wide maximum is 0.81 ppb and the domain-wide minimum is −1.33 ppb. The average ozone response to the ~13% NO_X reductions clearly delineate the average extent of the modeled VOC-sensitive versus NOx-sensitive chemical regimes within the SoCAB.

Figure 10b provides a closer look at the period-average CMAQ-predicted impacts of the COVID-19 emission reductions throughout the SoCAB, with monitor locations indicated. The area of ozone increases encompasses the southeastern quadrant of Los Angeles County and stretches into San Bernardino and Orange Counties. The area of ozone decreases occurs over a larger area that includes Santa Clarita Valley, most of San Bernardino, Riverside, and southern Orange Counties. Although the area of ozone decreases is larger than the area of ozone increases, a vast majority of the population resides in the area of ozone increases.

Table 3 reports the CMAQ-predicted period-average, period-maximum, and period-minimum MDA8 ozone differences at the SoCAB monitors (refer to Figure 8 for the locations of the monitors). Monitors with higher ozone on average in the 2020 COVID Case compared to the 2020 BAU Case are shown in red, and those with lower ozone are shown in blue. All monitors have higher ozone for at least one day in the June 1—July 31 period, with an ozone increase indicating that the NO_X disbenefits are not just limited to the SoCAB central urban areas. The maximum ozone increase at any monitor is at Glendora (2.77 ppb);

surprisingly, the monitoring site with the fourth highest ozone increase is Crestline at Lake Gregory, far downwind and in the San Bernardino Mountains, which is a site where ozone formation is usually more NO_X-sensitive.

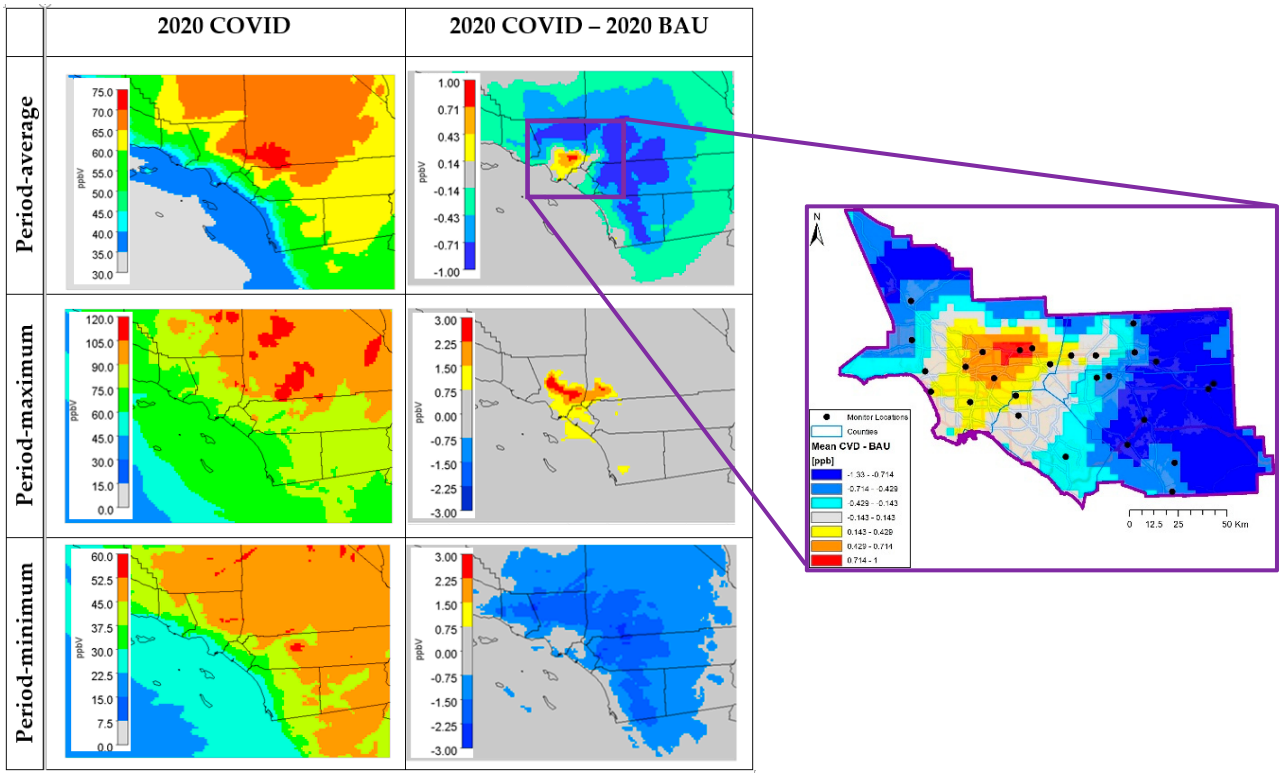

Figure 10. 1 June–31 July impacts of the COVID-19 emissions reductions on ozone, estimated by CMAQ: (**a**) Period-average, period-maximum, and period-minimum MDA8 ozone spatial maps for 2020 COVID and 2020 COVID minus 2020 BAU; (**b**) Close up of period-average 2020 COVID minus 2020 BAU for SoCAB.

For the period-minimum differences, all monitors have lower ozone for at least one day in the June 1–July 31 period. The largest ozone decreases with reductions of over −2 ppb occur at sites that tend to be the furthest downwind, such as Banning Airport (−2.3 ppb). Even at monitoring sites within central Los Angeles County where ozone formation is more VOC-sensitive, there is at least one day during the June–July 2020 episode where ozone is reduced due to the NO_x controls.

Table 3. CMAQ impacts of the ozone response to COVID-19 emissions reductions at the SOCAB monitors (2020 COVID—2020 BAU). Period mean, maximum, and minimum impact.

AQS Number	Monitor Name	Period-Average MDA8 Difference (ppb)	Period-Maximum MDA8 Difference (ppb)	Period-Minimum MDA8 Difference (ppb)
60370002	Azusa	0.80	2.72	−0.57
60370016	Glendora	0.77	2.77	−0.75
60370113	West Los Angeles	−0.04	0.46	−0.52
60371103	Los Angeles (Main St.)	0.46	1.17	−0.05
60371201	Reseda	−0.54	0.28	−1.45
60371302	Compton	0.27	0.98	−0.34

Table 3. *Cont.*

AQS Number	Monitor Name	Period-Average MDA8 Difference (ppb)	Period-Maximum MDA8 Difference (ppb)	Period-Minimum MDA8 Difference (ppb)
60371602	Pico Rivera #2	0.56	1.95	−0.31
60371701	Pomona	0.20	2.08	−1.06
60372005	Pasadena	0.55	1.98	−0.21
60375005	LAX Hastings	0.23	0.93	−0.28
60376012	Santa Clarita	−0.67	1.53	−1.70
60590007	Anaheim	0.03	1.03	−0.75
60592022	Mission Viejo	−0.26	0.74	−1.00
60595001	La Habra	0.29	1.15	−0.32
60650009	Pechanga	−0.59	0.10	−1.30
60650012	Banning Airport	−1.09	0.27	−2.30
60650016	Temecula	−0.69	0.07	−1.57
60651016	Morongo	−1.13	0.48	−2.19
60656001	Perris	−1.16	0.10	−1.98
60658001	Rubidoux	−0.50	0.72	−1.38
60658005	Mira Loma	−0.42	0.90	−1.31
60659001	Lake Elsinore	−1.04	0.01	−2.21
60710005	Crestline	−0.65	2.01	−2.15
60711004	Upland	0.10	1.88	−1.29
60712002	Fontana	0.05	1.72	−1.18
60714003	Redlands	−0.76	0.75	−1.74
60719004	San Bernardino	−0.58	1.27	−1.69

Red indicates increases and blue indicates decreases in period-average MDA8 ozone

4. Discussion

The dynamic model evaluation component of this study showed that, throughout much of the SoCAB, CMAQ can replicate the observed ozone response to the COVID-19 emissions reductions and changes in meteorology between 2019 and 2020 using the EPA's ozone projection procedures. The modeled ozone response was, however, generally weaker than observations. This is similar to the finding of Karamchandani et al. [15], who found the CMAQ model to be "stiff" (i.e., underpredicted the ozone response). Our results of the evaluation of the COVID-19 impacts with CMAQ showed variable ozone response to NOx reductions across the SoCAB, with an approximately 50 km × 50 km region in Los Angeles County that had average MDA8 ozone increases, and elsewhere throughout the SoCAB there were ozone decreases. This result agrees with regional modeling studies that use different air quality models and grid resolutions (e.g., Campbell et al. [6], Gaubert et al. [7], and Keller et al. [8]), which found similar variable ozone responses with localized increases in urban areas. This suggests that this phenomenon is robust to different air quality models at differing spatial scales.

This study is limited by a few factors: (1) relatively small COVID-19 emissions reductions (i.e., ~13% NOx); (2) limited spatial and temporal resolution for the emissions adjustments (i.e., no day-of-the-week effect for on-road adjustments); (3) non-COVID adjusted boundary conditions (COVID adjusted boundary conditions would account for regional and global background changes in ozone and ozone precursors transported into the SoCAB via boundary conditions); and (4) uncertainties in emissions, in particular, VOCs and biogenics. Regarding the third limitation, Bouarar et al. [32] investigated the response of chemical species in the free troposphere during the COVID-19 pandemic using the CAM-chem model and found zonally averaged ozone to be 5–15% lower than 19-year climatological values. Their modeling successfully reproduced the observed ozone anomalies during the 6 months that followed the COVID-19 outbreak that were presented in Steinbrecht et al. [33]. The 2020 anomaly compared to climatology was found to be primarily due to reduced air traffic, reduced surface emissions, and anomalous 2020 meteorology. It is unclear how potential longer-term trends were considered and accounted

for over the climatological period. Our future work will consider the impact of COVID-19 effects on free tropospheric ozone and transport from outside the SoCAB. Omission of a potential reduction in background ozone may plausibly contribute to the CMAQ model "stiffness" described above, but due to the non-linearity of ozone formation and because the SoCAB encompasses both VOC and NOx-sensitive regimes it is difficult to predict how the model would respond to combined changes (i.e., background ozone plus local emissions reductions) across the SoCAB; however, we note that our findings could change substantially under that scenario. Typically for model attainment demonstrations, such as the SCQMD 2016 AQMP [25], global BCs are held constant due to lack of accurate information to make an adjustment, and the analysis in this study is consistent with that approach. If future work shows substantial differences in modeled ozone responses due to background ozone, the effects of background ozone on model attainment demonstrations should be explored.

Recommendations for further study are as follows:

1. Obtain, evaluate, and utilize WACCM 2020 COVID impacted BCs for the 2020 COVID simulation. This will provide a more complete assessment of the COVID impacts and enable a comparison of the effect of local versus background COVID impacts;
2. A targeted NOx model evaluation and VOC evaluation;
3. A more rigorous WRF evaluation including an assessment of the marine layer;
4. Day-of-the-week adjustment to the on-road sector to allow for day-of-the-week analyses to provide additional insight into the current extent of VOC-limited versus NOx-limited chemical regimes.

5. Conclusions

1. The modeled ozone changes between 2019 and 2020 are generally consistent with the observed ozone changes using procedures that are used to make future-year ozone projections, which lends confidence in our future-year ozone projections;
2. Accounting for changes in background ozone in the free troposphere due to COVID-19 effects could substantially change our findings;
3. Although meteorology played the major role in the increases in ozone between 2019 and 2020, the reduction in NO_x emissions due to the response of the COVID pandemic also caused ozone increases in Los Angeles County and into western San Bernardino County, with more widespread ozone decreases further east;
4. Ozone formation in parts of the SoCAB is still VOC-sensitive, and the locations where NO_x reductions cause ozone increases occur in areas with some of the highest population density in the SoCAB;
5. The evaluation of VOC/NO_x emission control strategies to attain the ozone NAAQS needs to examine ozone levels in the intervening years between the current and the attainment year to better understand whether ozone may be getting worse or cause more population exposure to high ozone concentrations rather than focusing solely on ozone levels in the attainment year.

Supplementary Materials: The following supporting information can be downloaded at: https://www.mdpi.com/article/10.3390/atmos13040528/s1, A Supplementary Materials Document is available with additional supporting Materials. Section S1 is a WRF evaluation, Section S2 provides additional CMAQ specification, Section S3 lists emissions scaling methodologies, and Section S4 provides additional CMAQ operational model performance.

Author Contributions: Conceptualization, R.M., L.K.P. and J.J.; WRF modeling, J.J.; emissions inventories, J.G. and R.P.; CMAQ modeling and AMET postprocessing, P.V.; biogenic and fire emissions preparation, C.-J.C.; emissions processing L.K.P. and C.-J.C.; project coordination, L.K.P. and J.J.; analysis, L.K.P., R.M. and J.J.; visualizations, L.K.P. and P.V.; writing—original draft preparation, L.K.P.; writing—review and editing, R.M.; supervision, R.M.; funding acquisition, R.M. All authors have read and agreed to the published version of the manuscript.

Funding: This research was funded by the Coordinated Research Council (CRC) Contract Number A−126 and the Truck and Engine Manufacturer's Association (EMA).

Institutional Review Board Statement: Not applicable.

Informed Consent Statement: Not applicable.

Acknowledgments: We are grateful to Jeremy Avise at the California Air Resources (ARB) for the 2020 model-ready emissions inventories and the South Coast Air Quality Management District (SCAQMD) for providing 2016 AQMP modeling databases that were used in preliminary work.

Conflicts of Interest: The authors declare no conflict of interest.

References

1. Gkatzelis, G.I.; Gilman, J.B.; Brown, S.S.; Eskes, H.; Gomes, A.R.; Lange, A.C.; McDonald, B.C.; Peischl, J.; Petzold, A.; Thompson, C.R.; et al. The Global Impacts of COVID-19 Lockdowns on Urban Air Pollution: A Critical Review and Recommendations. *Elem. Sci. Anthr.* **2021**, *9*, 00176. Available online: https://online.ucpress.edu/elementa/article/9/1/00176/116616/The-global-impacts-of-COVID-19-lockdowns-on-urban (accessed on 10 May 2021). [CrossRef]
2. Bekbulat, B.; Apte, J.S.; Millet, D.B.; Robinson, A.L.; Wells, K.C.; Presto, A.A.; Marshall, J.D. Changes in Criteria Air Pollution Levels in the US before, during, and after Covid-19 Stay-at-Home Orders: Evidence from Regulatory Monitors. *Sci. Total Environ.* **2021**, *769*, 144693. Available online: https://www.sciencedirect.com/science/article/pii/S0048969720382267 (accessed on 10 May 2021). [CrossRef] [PubMed]
3. Fu, F.; Purvis-Roberts, K.L.; Williams, B. Impact of the COVID-19 pandemic lockdown on air pollution in 20 major cities around the world. *Atmosphere* **2020**, *11*, 1189. [CrossRef]
4. Goldberg, D.L.; Anenberg, S.C.; Griffin, D.; McLinden, C.A.; Lu, Z.; Streets, D.G. Disentangling the impact of the COVID-19 lockdowns on urban NO2 from natural variability. *Geophys. Res. Lett.* **2020**, *47*, e2020GL089269. [CrossRef]
5. Venter, Z.S.; Aunan, K.; Chowdhury, S.; Lelieveld, J. COVID-19 lockdowns cause global air pollution declines. *Proc. Natl. Acad. Sci. USA* **2020**, *117*, 18984–18990. [CrossRef] [PubMed]
6. Campbell, P.C.; Tong, D.; Tang, Y.; Baker, B.; Lee, P.; Saylor, R.; Stein, A.; Ma, S.; Lamsal, L.; Qu, Z. Impacts of the COVID-19 Economic Slowdown on Ozone Pollution in the U.S. *Atmos. Environ.* **2021**, *264*, 118713. Available online: https://www.sciencedirect.com/science/article/pii/S1352231021005355 (accessed on 5 March 2022). [CrossRef] [PubMed]
7. Gaubert, B.; Bouarar, I.; Doumbia, T.; Liu, Y.; Stavrakou, T.; Deroubaix, A.; Darras, S.; Elguindi, N.; Granier, C.; Lacey, F.; et al. Global changes in secondary atmospheric pollutants during the 2020 COVID-19 pandemic. *J. Geophys. Res. Atmos.* **2021**, *126*, e2020JD034213. [CrossRef]
8. Keller, C.A.; Evans, M.J.; Knowland, K.E.; Hasenkopf, C.A.; Modekurty, S.; Lucchesi, R.A.; Oda, T.; Franca, B.B.; Mandarino, F.C.; Díaz Suárez, M.V.; et al. Global impact of COVID-19 restrictions on the surface concentrations of nitrogen dioxide and ozone. *Atmos. Chem. Phys.* **2021**, *21*, 3555–3592. [CrossRef]
9. Ivey, C.; Gao, Z.; Do, K.; Kashfi Yeganeh, A.; Russell, A.; Blanchard, C.L.; Lee, S.M. Impacts of the 2020 COVID-19 Shutdown Measures on Ozone Production in the Los Angeles Basin. *ChemRxiv.* **2020**. [CrossRef]
10. Parker, H.A.; Hasheminassab, S.; Crounse, J.D.; Roehl, C.M.; Wennberg, P.O. Impacts of traffic reductions associated with COVID-19 on Southern California air quality. *Geophys. Res. Lett.* **2020**, *47*, e2020GL090164. [CrossRef] [PubMed]
11. Community Multiscale Air Quality. Available online: https://www.epa.gov/cmaq (accessed on 28 February 2022).
12. Dennis, R.; Fox, T.; Fuentes, M.; Gilliland, A.; Hanna, S.; Hogrefe, C.; Irwin, J.; Rao, S.T.; Scheffe, R.; Schere, K.; et al. A framework for evaluating regional-scale numerical photochemical modeling systems. *Environ. Fluid Mech.* **2010**, *10*, 471–489. [CrossRef] [PubMed]
13. USEPA. Atmospheric Model Evaluation Tool. Available online: https://www.epa.gov/cmaq/atmospheric-model-evaluation-tool (accessed on 10 April 2021).
14. USEPA. Modeling Guidance for Demonstrating Air Quality Goals for Ozone, PM2.s and Regional Haze, Memorandum from Richard A. Wayland. 2018. Available online: https://www.epa.gov/sites/default/files/2020-10/documents/o3-pm-rh-modeling_guidance-2018.pdf (accessed on 10 April 2021).
15. Karamchandani, P.; Morris, R.; Wentland, A.; Shah, T.; Reid, S.; Lester, J. Dynamic evaluation of photochemical grid model response to emission changes in the South Coast Air Basin in California. *Atmosphere* **2017**, *8*, 145. [CrossRef]
16. Google. COVID-19 Community Mobility Reports. Available online: https://www.google.com/covid19/mobility/ (accessed on 1 October 2020).
17. NASA. Los Angeles OMI Data. Available online: https://so2.gsfc.nasa.gov/no2/pix/htmls/Los_Angeles_data.html (accessed on 1 October 2020).
18. Goldberg, D. *Milken Institute School of Public Health*; Personal Communication: Washington, DC, USA, 2021.
19. Qu, Z.; Jacob, D.J.; Silvern, R.F.; Shah, V.; Campbell, P.C.; Valin, L.C.; Murray, L.T. US COVID-19 shutdown demonstrates importance of background NO_2 in inferring NO_x emissions from satellite NO_2 observations. *Geophys. Res. Lett.* **2021**, *48*, e2021GL092783. [CrossRef] [PubMed]

20. CalFire. 2020 California Wildfire Incident Archive. Available online: https://www.fire.ca.gov/incidents/2020/ (accessed on 12 December 2021).
21. USEPA. Meteorology—Chemistry Interface Processor (MCIP). Available online: https://www.epa.gov/cmaq/meteorology-chemistry-interface-processor (accessed on 15 January 2020).
22. Avise, J. *California Air Resources Board*; Personal Communication: Sacramento, CA, USA, 2021.
23. University of California, Irvine, Biosphere Atmosphere Interactions Group. Model of Emissions of Gases and Aerosols from Nature (MEGAN) v3.1. Available online: https://bai.ess.uci.edu/megan (accessed on 20 October 2019).
24. National Center for Atmospheric Research (NCAR). Fire Inventory from NCAR (FINN). Available online: https://www2.acom.ucar.edu/modeling/finn-fire-inventory-ncar (accessed on 1 September 2021).
25. South Coast Air Quality Management District. Final 2016 Air Quality Management Plan. Available online: http://www.aqmd.gov/docs/default-source/clean-air-plans/air-quality-management-plans/2016-air-quality-management-plan/final-2016-aqmp/final2016aqmp.pdf?sfvrsn=15 (accessed on 9 August 2017).
26. California Air Resources Board; CEPAM. 2016 SIP—Standard Emissions Tool. Available online: https://www.arb.ca.gov/app/emsinv/fcemssumcat/fcemssumcat2016.php (accessed on 10 August 2021).
27. California Air Resources Board. Emission FACtor (EMFAC) Tool. Available online: https://arb.ca.gov/emfac/ (accessed on 1 September 2021).
28. National Center for Atmospheric Research (NCAR). Whole Atmosphere Community Climate Model (WACCM). Available online: https://www2.acom.ucar.edu/gcm/waccm (accessed on 5 September 2021).
29. Emery, C.E.; Liu, Z.; Russell, A.G.; Odman, M.T.; Yarwood, G.; Kumar, N. Recommendations on Statistics and Benchmarks to Assess Photochemical Model Performance. *J Air Waste Manag Assoc.* **2016**, *67*, 582–598. Available online: https://www.tandfonline.com/doi/full/10.1080/10962247.2016.1265027 (accessed on 5 November 2021). [CrossRef] [PubMed]
30. Dickerson, R.R.; Anderson, D.C.; Ren, X. On the Use of Data from Commercial NOx Analyzers for Air Pollution Studies. *Atmos. Environ.* **2019**, *215*, 116873. Available online: https://doi.org/10.1016/j.atmosenv.2019.116873 (accessed on 8 November 2021). [CrossRef]
31. Toro, C.; Foley, K.; Simon, H.; Henderson, B.; Baker, K.; Eyth, A.; Timin, B.; Appel, W.; Luecken, D.; Beardsley, M.; et al. Evaluation of 15 years of modeled atmospheric oxidized nitrogen compounds across the contiguous United States. *Elem. Sci. Anthr.* **2021**, *9*, 00158. [CrossRef] [PubMed]
32. Bouarar, I.; Gaubert, B.; Brasseur, G.P.; Steinbrecht, W.; Doumbia, T.; Tilmes, S.; Liu, Y.; Stavrakou, T.; Deroubaix, A.; Darras, S.; et al. Ozone anomalies in the free troposphere during the COVID-19 pandemic. *Geophys. Res. Lett.* **2021**, *8*, e2021GL094204. [CrossRef]
33. Steinbrecht, W.; Kubistin, D.; Plass-Dulmer, C.; Davies, J.; Tarasick, D.W.; von der Gathen, P.; Deckelmann, H.; Jepsen, N.; Kivi, R.; Lyall, N.; et al. COVID-19 crisis reduces free tropospheric ozone across the Northern Hemisphere. *Geophys. Res. Lett.* **2021**, *48*, e2020GL091987. [CrossRef]